

STABILIZED FINITE ELEMENT METHODS IN FLUIDS: INSPIRATIONS, ORIGINS, STATUS AND RECENT DEVELOPMENTS

T. J. R. Hughes, G. Hauke and K. Jansen
*Stanford University,
Stanford, California
USA*

Z. Johan
*Thinking Machines Co.
Paris
France*

ABSTRACT

Stabilized finite element methods were inspired by the search for an explanation of methods which did not emanate from the Galerkin recipe. The earliest useful applications from an engineering viewpoint concerned fluids and this remains the most thoroughly developed. We review the current status of stabilized methods in fluids from the perspectives of methodology and algorithms. We also present summaries of some recent developments, namely, methods which allow the use of arbitrary variable sets in fluids and provide a unified framework for incompressible and compressible flows; initial applications to turbulent flows; and considerations of massively parallel computing.

1. INTRODUCTION

Finite element methods have been applied to fluid dynamics problems for some time now. The early work focused on Galerkin's method and various attempts to improve its stability while retaining its basic character. The first of a new class of methods was developed in the late 1970's, namely, "SUPG." SUPG has been shown to possess a unique combination of accuracy and stability. From the current perspective, SUPG is just an example of a general class of methods possessing good accuracy and stability properties. These have become known as "stabilized methods." Another stabilized method which has found applicability in computational fluid mechanics is Galerkin/least-squares, or "GLS" for short. In the next section we review and summarize the status of currently employed methods and algorithms.

In preparing this paper, the senior author was reminded that the seeds of stabilized methods were planted in the early 1970's during the days he worked with Professor Robert L. Taylor at Berkeley. Two examples of superior methods in structural mechanics which did not arise from the Galerkin recipe spurred a search for a more general finite element framework. The examples involved what was referred to as "higher-order mass matrices." They are described on pages 446-447 of [21]. The original references are [1,2,3]. It is possible to derive these methods from the viewpoint of stabilized methods. So far, however, stabilized methods have been most thoroughly developed in the context of fluid mechanics. There have been only a small number of papers applying stabilized methods to structural mechanics. This area remains a fruitful one for future developments.

Stabilized methods were initially developed for the practically important area of incompressible flows in [4] and later extended to compressible flows [5-8]. Our work in compressible flows has emphasized the use of entropy variables. Although the method based on entropy variables possesses unique properties, it is very appealing to extend the formulation to other sets of variables, such

as primitive variables. Hughes and Tezduyar [9], Hansbo and Johnson [10] and Aliabadi, Ray and Tezduyar [11] have already developed similar methods within the context of conservation variables. Possible benefits of the availability of the various formulations include easier implementation within existing codes and extension of the range of turbulence models that can be used. The use of primitive variables (p, \mathbf{u}, T), or entropy variables, also allows the solution of incompressible and compressible flows within the same program. We present a new formulation herein which permits the use of any set of variables. It is conservative and attains correct shock structure for any choice of variables.

The success of stabilized finite element methods for the laminar Navier-Stokes equations has motivated extension to turbulent flows. We consider Reynolds-averaged systems which include a turbulent kinetic energy transport equation (“one-equation models”). We identify a turbulent entropy production (in)equality associated with such systems and show that it may be automatically embedded within our numerical formulation, thus incorporating the fundamental nonlinear stability condition *ab initio*.

We also present a few numerical calculations illustrating the preceding ideas. In addition, we present applications on massively parallel computers. We briefly illustrate issues of load balancing via a parallelized domain decomposition algorithm and present timings for a supersonic aerodynamic calculation on a contemporary platform, the Connection Machine CM-5.

2. STABILIZED METHODS

We begin with a review of the fundamental methodologies and algorithmic procedures which we employ.

2.1 Fundamental methodologies

1. *Symmetric advective diffusive systems* can be written as

$$\tilde{\mathbf{A}}_0 \mathbf{V}_{,t} + \tilde{\mathbf{A}}_i \mathbf{V}_{,i} = (\tilde{\mathbf{K}}_{ij} \mathbf{V}_{,j})_{,i} + \tilde{\mathcal{F}} \quad (1)$$

where

$$\begin{aligned} \tilde{\mathbf{A}}_0(\mathbf{V}) &= \partial \mathbf{U} / \partial \mathbf{V} && \text{symmetric, positive-definite} \\ \tilde{\mathbf{A}}_i(\mathbf{V}) &= \partial \mathbf{F}_i^{\text{adv}} / \partial \mathbf{V} && \text{symmetric} \\ \tilde{\mathbf{K}}(\mathbf{V}) &= [\tilde{\mathbf{K}}_{ij}] && \text{symmetric, positive-semidefinite} \\ \mathbf{F}_i^{\text{diff}} &= \tilde{\mathbf{K}}_{ij} \mathbf{V}_{,j} \end{aligned}$$

which is a quasi-linearization of the conservative form of the system

$$\mathbf{U}_{,t} + \mathbf{F}_{i,i}^{\text{adv}} = \mathbf{F}_{i,i}^{\text{diff}} + \mathcal{F} \quad (2)$$

where \mathbf{U} is the vector of conserved variables, $\mathbf{F}_i^{\text{adv}}$ is the advective flux in the i^{th} -direction, $\mathbf{F}_i^{\text{diff}}$ is the diffusive flux in the i^{th} -direction, and \mathcal{F} is the source vector.

(1) provides a unified framework for diverse classes of flow phenomena and also an intimate link with the nonequilibrium thermodynamical foundations of fluid mechanical systems. Methods developed for such systems have wide applicability, see e.g. Hughes *et al.* [5,8,12].

2. *Entropy variables*, described by de Groot and Mazur [13], transform fluid dynamical systems to canonical symmetric advective-diffusive form, and lead to automatic, discrete entropy production for appropriately constructed finite element methods. This amounts to the fundamental nonlinear stability condition of the underlying theory, see Hughes *et al.* [5].
3. *Unstructured space-time discretizations* (see Figure 1), advocated by Johnson [14], unify and extend notions such as arbitrary Lagrangian-Eulerian methods (ALE), free Lagrangian methods, and methods based on characteristics and/or Riemann solvers involving accurate transport plus projection from one mesh to another.

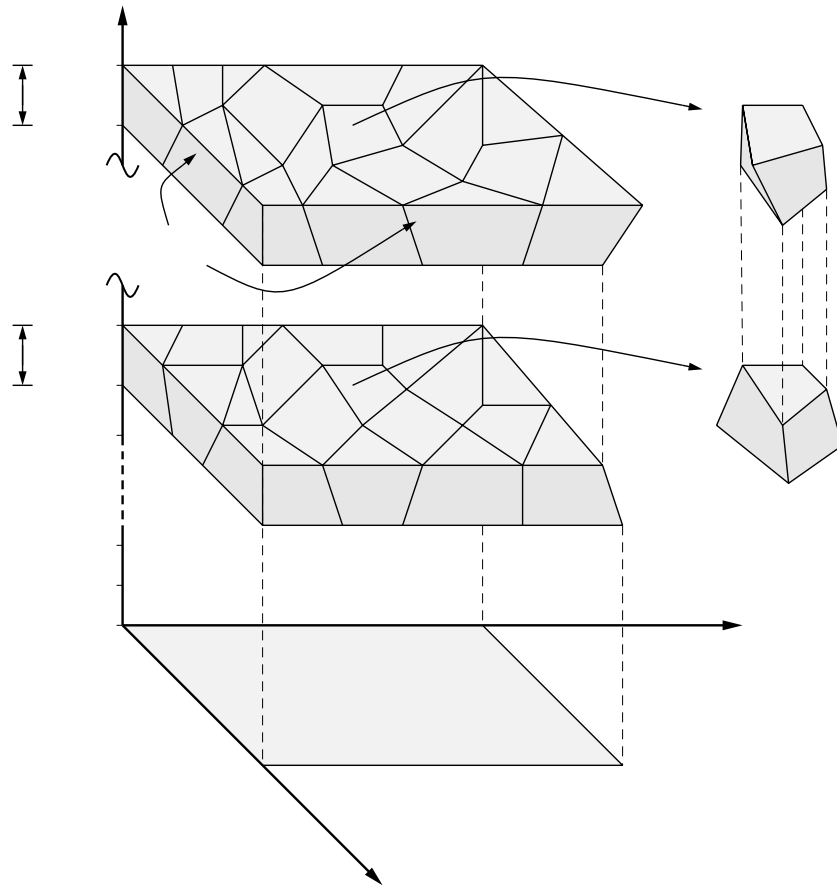


Figure 1. Unstructured space-time discretization of successive time slabs.

4. *Discontinuous Galerkin method in time*, introduced by Lesaint and Raviart [15] in the context of neutron transport, serves as the basis for the variational formulation and is represented here by

$$\begin{aligned}
0 = & \int_{Q_n} \left(-\mathbf{W}_{,t} \cdot \mathbf{U}(\mathbf{V}) - \mathbf{W}_{,i} \cdot \mathbf{F}_i^{\text{adv}}(\mathbf{V}) + \mathbf{W}_{,i} \cdot \mathbf{F}_i^{\text{diff}}(\mathbf{V}) - \mathbf{W} \cdot \tilde{\mathcal{F}} \right) dQ \\
& + \int_{\Omega} \left(\mathbf{W}(t_{n+1}^-) \cdot \mathbf{U}(\mathbf{V}(t_{n+1}^-)) - \mathbf{W}(t_n^+) \cdot \mathbf{U}(\mathbf{V}(t_n^-)) \right) d\Omega \quad (3) \\
& - \int_{P_n} \mathbf{W} \cdot \left(-\mathbf{F}_i^{\text{adv}}(\mathbf{V}) + \mathbf{F}_i^{\text{diff}}(\mathbf{V}) \right) n_i dP
\end{aligned}$$

5. *Stabilized methods.* Stabilizing terms are a necessary addition to (3) since the Galerkin formulation is known to possess poor stability. In the Galerkin/least-squares method, the term

$$+ \sum_{e=1}^{(n_{el})_n} \int_{Q_n^e} \left(\tilde{\mathcal{L}}\mathbf{W} \right) \cdot \tilde{\tau} \left(\tilde{\mathcal{L}}\mathbf{V} - \tilde{\mathcal{F}} \right) dQ \quad (4)$$

is added to (3) to provide least-squares control of the *residual*, which is a computable measure of the error in a finite element method. This concept does not exist in finite difference methods. Here

$$\tilde{\mathcal{L}} = \tilde{\mathbf{A}}_0 \frac{\partial}{\partial t} + \tilde{\mathbf{A}}_i \frac{\partial}{\partial x_i} - \frac{\partial}{\partial x_i} \left(\tilde{\mathbf{K}}_{ij} \frac{\partial}{\partial x_j} \right) \quad (5)$$

and $\tilde{\tau}$ is an $m \times m$ symmetric positive-semidefinite matrix of intrinsic time scales (see Hughes and Mallet [6]).

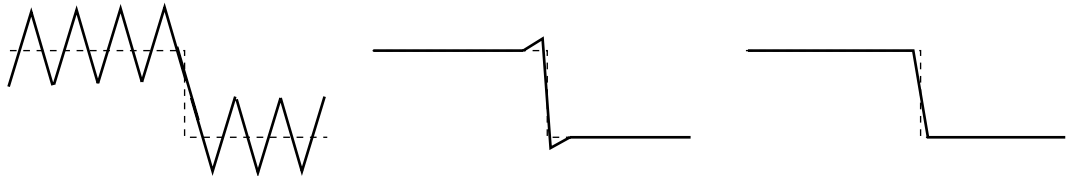


Figure 2. Oscillations present in Galerkin's method (left) are controlled by stabilized methods (middle), and remaining overshoots/undershoots are removed by the discontinuity capturing operator (right).

6. *Nonlinear discontinuity capturing operators* are residual-based, nonlinear viscosities, which control solution behavior about discontinuities and sharp layers. A typical form is

$$+ \sum_{e=1}^{(n_{el})_n} \int_{Q_n^e} \tilde{\nu}^h g^{ij} \mathbf{W}_{,i} \cdot \tilde{\mathbf{A}}_0 \mathbf{V}_{,j} dQ \quad (6)$$

$$\begin{bmatrix} & & & \\ \square & & & \\ & \square & & \\ & & \square & \\ & & & \ddots \\ & & & & \square \end{bmatrix}$$

Figure 3. Nodal block-diagonal matrix.

where

$$\tilde{\nu}^h = \frac{2|\tilde{\mathcal{L}}\mathbf{V}^h - \tilde{\mathcal{F}}|_{\tau}^2}{g^{ij}\mathbf{V}_{,i} \cdot \tilde{\mathbf{A}}_0 \mathbf{V}_{,j}} \quad (7)$$

and

$$g^{ij} = [\xi_{k,i}\xi_{k,j}]^{-1} \quad (8)$$

Note that the viscosity (7) depends on the square of the residual and is therefore small when the residual is small, i.e., when resolution is adequate. Stabilization terms, such as (4) and (6) clarify and extend fundamental concepts originated by Von Neumann and Richtmyer [16], namely that of linear and nonlinear artificial diffusion. The important difference here is that our artificial diffusion terms attack residuals, i.e., errors, not features and therefore vanish in regions of adequate resolution. The upshot is a unique combination of accuracy *and* stability. This has been shown mathematically and verified numerically, and results in a fundamental solution to the basic problem of computational fluid dynamics, namely, combining good accuracy and stability in one method. Figure 2 schematically illustrates the effects of the different ingredients in the variational formulation when a solution possesses a discontinuity.

2.2 Algorithmic procedures

1. *Predictor-(multi)corrector algorithms* are useful for time accurate calculations. These methods have been traditionally used to achieve high accuracy in explicit calculations. Implicit space-time methods also benefit from these concepts. Predictor-multicorrector algorithms can reduce the size of the resulting implicit system while retaining higher-order accuracy; see Shakib *et al.* [17].
2. *The generalized minimal residual (GMRES) algorithm* is an iterative solution procedure which constructs a Krylov space within which to minimize the residual of the solution

$$\mathbf{A}(\mathbf{u})\mathbf{p} = \mathbf{R}(\mathbf{u}) \quad (9)$$

Each Krylov vector requires a matrix-vector product. Compressible flows are well suited to this type of algorithm as is evident by the size of the Krylov space required, typically less than 15, see Shakib *et al.* [18].

3. *Nodal block-diagonal preconditioning.* Figure 3 schematically illustrates the structure of a nodal block-diagonal matrix. The nodal block-diagonal submatrix of the implicit operator is employed as a preconditioner. This has been shown to significantly improve convergence.

4. *Element-by-element data structures* are exploited in the following ways:

- Preconditioning is performed more efficiently by utilizing the element-by-element data structure. Two forms of element-by-element preconditioning have been studied by Shakib *et al.* [17,18], nonsymmetric Cholesky and Gauss-Seidel. Gauss-Seidel has been shown to improve performance without engendering additional storage.
- Matrix-vector products can be performed very efficiently in element-by-element fashion without storing the assembled matrix; see Figure 4.

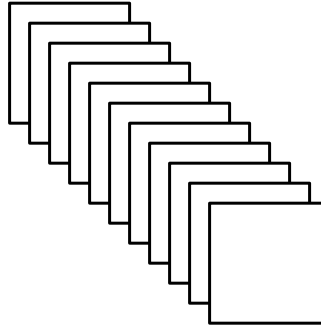


Figure 4. Element-by-element data structures obviate the need to store global matrices.

5. *The matrix-free (GMRES) algorithm* eliminates the need for matrix representation in the matrix-vector product. The matrix-vector product can be approximated by residual evaluations, i.e.,

$$\mathbf{A}(\mathbf{u})\mathbf{p} = \frac{\mathbf{R}(\mathbf{u} + \epsilon\mathbf{p}) - \mathbf{R}(\mathbf{u})}{\epsilon} \quad (10)$$

This reduces memory requirements, especially in three dimensions; see Johan *et al.* [19].

- 6. *Multi-element group domain decomposition* allows problems to be partitioned for parallelization so that different solvers, such as explicit or implicit, can be used in different regions, see Shakib *et al.* [17].
- 7. *Parallel implementations* make use of a two-level domain decomposition. The coarse level is suitable for localizing data on processing nodes. The fine level maximizes vectorization and computational efficiency on processing nodes. The quality of the decomposition can significantly lessen communication costs; see Johan *et al.* [20].

3. A GLS FORMULATION FOR ANY SET OF VARIABLES

Entropy variables are but one of many variables choices. Using any independent set of variables \mathbf{Y} , it is possible to rewrite (2) in a general quasi-linear form as

$$\mathbf{A}_0 \mathbf{Y}_{,t} + \mathbf{A}_i \mathbf{Y}_{,i} = (\mathbf{K}_{ij} \mathbf{Y}_{,j})_{,i} + \mathcal{F} \quad (11)$$

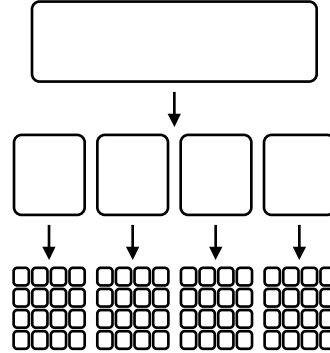


Figure 5. Two-level domain decomposition for parallel implementations.

where $\mathbf{A}_0 = \mathbf{U}_{,\mathbf{Y}}$, $\mathbf{A}_i = \mathbf{F}_{i,\mathbf{Y}}^{\text{adv}}$ is the i^{th} Euler Jacobian matrix, and $\mathbf{K} = [\mathbf{K}_{ij}]$ is the diffusivity matrix where $\mathbf{K}_{ij}\mathbf{Y}_{,j} = \mathbf{F}_i^{\text{diff}}$.

Having discussed the method for entropy variables, we apply the chain rule,

$$\mathbf{V}_{,i} = \mathbf{V}_{,\mathbf{Y}}\mathbf{Y}_{,i} \quad (12)$$

to obtain the conservation laws in any variable set. The coefficient matrices transform according to

$$\begin{aligned} \widetilde{\mathbf{A}}_0 \mathbf{V}_{,\mathbf{Y}} &= \mathbf{A}_0 \\ \widetilde{\mathbf{A}}_i \mathbf{V}_{,\mathbf{Y}} &= \mathbf{A}_i \\ \widetilde{\mathbf{K}}_{i,j} \mathbf{V}_{,\mathbf{Y}} &= \mathbf{K}_{ij} \end{aligned} \quad (13)$$

Thus, changing variables under the integral sign, the weak form (2,3,5) can be rewritten as follows: Within each Q_n , $n = 0, \dots, N - 1$, find $\mathbf{Y} \in \mathcal{S}_{\mathbf{Y}}$ such that $\forall \mathbf{W} \in \mathcal{V}_{\mathbf{Y}}$:

$$\begin{aligned} &\int_{Q_n} \left(-\mathbf{W}_{,t} \cdot \mathbf{U}(\mathbf{Y}) - \mathbf{W}_{,i} \cdot \mathbf{F}_i^{\text{adv}}(\mathbf{Y}) + \mathbf{W}_{,i} \cdot \mathbf{K}_{ij} \mathbf{Y}_{,j} - \mathbf{W} \cdot \mathcal{F} \right) dQ \\ &+ \int_{\Omega} \left(\mathbf{W}(t_{n+1}^-) \cdot \mathbf{U}(\mathbf{Y}(t_{n+1}^-)) - \mathbf{W}(t_n^+) \cdot \mathbf{U}(\mathbf{Y}(t_n^-)) \right) d\Omega \\ &+ \sum_{e=1}^{(n_{\text{el}})_n} \int_{Q_n^e} \left(\mathcal{L}^T \mathbf{W} \right) \cdot \boldsymbol{\tau} \left(\mathcal{L} \mathbf{Y} - \mathcal{F} \right) dQ \\ &+ \sum_{e=1}^{(n_{\text{el}})_n} \int_{Q_n^e} \nu^h g^{ij} \mathbf{W}_{,i} \cdot \mathbf{A}_0 \mathbf{Y}_{,j} dQ \\ &= \int_{P_n} \mathbf{W} \cdot \left(-\mathbf{F}_i^{\text{adv}}(\mathbf{Y}) + \mathbf{F}_i^{\text{diff}}(\mathbf{Y}) \right) n_i dP \end{aligned} \quad (14)$$

where $\mathcal{S}_{\mathbf{Y}}$ and $\mathcal{V}_{\mathbf{Y}}$ are typical finite element spaces.

The first and last integrals constitute the Galerkin terms expressed as a function of the variables \mathbf{Y} . The jump term remains essentially unchanged. The least-squares contribution is written in terms of the differential operator \mathcal{L} , which is given by

$$\mathcal{L} = \mathbf{A}_0 \frac{\partial}{\partial t} + \mathbf{A}_i \frac{\partial}{\partial x_i} - \frac{\partial}{\partial x_i} (\mathbf{K}_{ij} \frac{\partial}{\partial x_j}) \quad (15)$$

and \mathcal{L}^T , which is defined by

$$\mathcal{L}^T = \mathbf{A}_0^T \frac{\partial}{\partial t} + \mathbf{A}_i^T \frac{\partial}{\partial x_i} - \frac{\partial}{\partial x_i} (\mathbf{K}_{ij}^T \frac{\partial}{\partial x_j}) \quad (16)$$

Note that when entropy variables are used, $\mathcal{L}^T = \mathcal{L}$ and (2,3,5) is recovered. The expression for $\boldsymbol{\tau}$, namely

$$\boldsymbol{\tau} = \mathbf{Y}, \mathbf{V} \tilde{\boldsymbol{\tau}} \quad (17)$$

neglects the spatial derivative of \mathbf{V}, \mathbf{Y} emanating from the diffusion term. In SUPG, the diffusion term's action on the weighting function in the least-squares contribution is omitted. Finally, the coefficient of the discontinuity capturing operator transforms in a similar fashion, i.e.,

$$\nu^h = \frac{2|\mathcal{L}\mathbf{V}^h - \mathcal{F}|_{\tilde{\boldsymbol{\tau}}}^2}{g^{ij} \mathbf{Y},_i \cdot \mathbf{V}_{,\mathbf{Y}}^T \tilde{\mathbf{A}}_0 \mathbf{V}, \mathbf{Y} \mathbf{Y},_j} \quad (18)$$

Remarks

- i) In general, the matrices \mathbf{A}_0 , \mathbf{A}_i and $\mathbf{K} = [\mathbf{K}_{ij}]$ are not symmetric.
- ii) The finite element method (14) is globally conservative (see [8]) and maintains correct shock structure.
- iii) The choice $\mathbf{Y} = \mathbf{V}$ (entropy variables) results in satisfaction of the entropy production (in)equality for the discrete solution without the additional dissipative mechanisms, namely, the least-squares and discontinuity capturing terms. For $\mathbf{Y} \neq \mathbf{V}$, entropy production is contingent upon the presence of these terms.
- iv) It is interesting to note that the incompressible limit is well defined for entropy variables and the “pressure” primitive variables (p, \mathbf{u}, T) , but not for conservation variables and the “density” primitive variables (ρ, \mathbf{u}, T) . Of particular interest among all possible sets of variables are the primitive variables (p, \mathbf{u}, T) . These have the greatest potential for efficient implementation due to the sparseness of coefficient matrices. For analogous considerations in classical elasticity see Hughes [21], Chapter 4.

4. A FEM FOR COMPRESSIBLE AND INCOMPRESSIBLE FLOWS

The quasi-linear form of the Navier-Stokes equations (11) depends on the equation of state of the fluid. In particular, an incompressible fluid can be considered as a divariant fluid which is characterized by constant density with the equation of state

$$de = c_v dT \quad (19)$$

where the specific heat is a given function of the temperature, i.e., $c_v = c_v(T)$. If the quasi-linear form of the Navier-Stokes equations is expressed in terms of entropy or pressure primitive variables, the assumed equation of state can be directly substituted in the coefficient matrices and the incompressible limit can be shown to exist. In this way, method (14) becomes a new technique for computing incompressible flows.

Remarks

- i) In the incompressible case, the matrix \mathbf{A}_0 is only positive-semidefinite.
- ii) This method accommodates thermally coupled and isothermal incompressible flows. Thermally coupled incompressible flows are obtained by allowing the viscosity to depend on the temperature. Isothermal incompressible flows can be obtained by specifying a constant viscosity.
- iii) The Boussinesq approximation may be attained by allowing the density to be temperature-dependent in the body force term.

5. THE REYNOLDS-AVERAGED NAVIER-STOKES EQUATIONS

The above methodologies have been recently extended to the Reynolds-averaged Navier-Stokes equations. When combined with a transport equation for the turbulent kinetic energy velocity scale q , these form a system of equations of the type presented in equation (2), namely

$$\mathbf{U}_{,t} + \mathbf{F}_{i,i}^{\text{adv}} = \mathbf{F}_{i,i}^{\text{diff}} + \mathcal{F} \quad (20)$$

where

$$\mathbf{U} = \left\{ \begin{array}{c} U_1 \\ U_2 \\ U_3 \\ U_4 \\ U_5 \\ U_6 \end{array} \right\} = \bar{\rho} \left\{ \begin{array}{c} 1 \\ \tilde{u}_1 \\ \tilde{u}_2 \\ \tilde{u}_3 \\ \tilde{e} + |\tilde{\mathbf{u}}|^2/2 + q^2/2 \\ q \end{array} \right\} \quad (21)$$

Bars and tildes over scalar variables denote standard ensemble averaging and Favre ensemble averaging, respectively. The reader should not confuse the averaging tildes with the matrix notation from previous section. See Favre [22], Vandromme [23] and Jansen *et al.* [24] for further details.

Next consider the generalized entropy function \mathcal{H} ,

$$\mathcal{H} = \mathcal{H}(\mathbf{U}) = -\bar{\rho}\hat{s}(\mathbf{U}) \quad (22)$$

where \hat{s} is the entropy calculated through the Gibbs relation in terms of the ensemble averaged variables present in our system, i.e., $\bar{\rho}$, \bar{p} and \tilde{T} . Introducing a change of variables $\mathbf{U} \mapsto \mathbf{V}$ defined by

$$\mathbf{V}^T = \frac{\partial \mathcal{H}}{\partial \mathbf{U}} \quad (23)$$

results in

$$\mathbf{V} = \frac{1}{\tilde{T}} \left\{ \begin{array}{c} \hat{\mu} - |\tilde{\mathbf{u}}|^2/2 - q^2/2 \\ \tilde{u}_1 \\ \tilde{u}_2 \\ \tilde{u}_3 \\ -1 \\ q \end{array} \right\} \quad (24)$$

where $\hat{\mu} = \tilde{e} + \bar{p}/\bar{\rho} - \tilde{T}\hat{s}$ is the turbulent electrochemical potential per unit mass. These variables, (24), are the entropy variables for the turbulent case. The advective-diffusive system can be converted to the quasi-linear form (1), namely,

$$\tilde{\mathbf{A}}_0 \mathbf{V}_{,t} + \tilde{\mathbf{A}}_i \mathbf{V}_{,i} = (\tilde{\mathbf{K}}_{ij} \mathbf{V}_{,j})_{,i} + \tilde{\mathcal{F}} \quad (25)$$

where $\tilde{\mathcal{F}} = \tilde{\mathcal{F}}(\mathbf{V}, \nabla \mathbf{V})$ is a nonlinear source term. The matrices retain the properties enjoyed by their unaveraged counterparts, namely: $\tilde{\mathbf{A}}_0$ is symmetric positive-definite; the $\tilde{\mathbf{A}}_i$'s are symmetric; and $\tilde{\mathbf{K}} = [\tilde{\mathbf{K}}_{ij}]$ is symmetric positive-semidefinite.

Furthermore, the system of equations can be shown to satisfy an entropy production (in)equality analogous to the Clausius-Duhem (in)equality for the unaveraged Navier-Stokes equations. Consider the dot product of \mathbf{V} with (25)

$$\mathbf{V} \cdot [\tilde{\mathbf{A}}_0 \mathbf{V}_{,t} + \tilde{\mathbf{A}}_i \mathbf{V}_{,i} = (\tilde{\mathbf{K}}_{ij} \mathbf{V}_{,j})_{,i} + \tilde{\mathcal{F}}] \quad (26)$$

Applying the product rule to the diffusivity term and rearranging yields

$$\mathbf{V} \cdot \tilde{\mathbf{A}}_0 \mathbf{V}_{,t} + \mathbf{V} \cdot \mathbf{F}_{i,i}^{\text{adv}} - (\mathbf{V} \cdot \mathbf{F}_i^{\text{diff}})_{,i} - \mathbf{V} \cdot \tilde{\mathcal{F}} = -\mathbf{V}_{,i} \cdot \tilde{\mathbf{K}}_{ij} \mathbf{V}_{,j} \quad (27)$$

Setting $\mathcal{H} = -\bar{\rho}\hat{s}$ in (27) leads to a Clausius-Duhem like (in)equality which governs turbulent entropy production for the system:

$$(\bar{\rho}\hat{s})_{,t} + (\bar{\rho}\hat{s}\tilde{u}_i)_{,i} + \left(\frac{-(\kappa + \kappa_T)\tilde{T}_{,i}}{\tilde{T}} \right)_{,i} = \frac{\Upsilon(\tilde{\mathbf{u}}, \tilde{\mathbf{u}})}{\tilde{T}} + (\kappa + \kappa_T) \frac{\tilde{T}_{,i}\tilde{T}_{,i}}{\tilde{T}^2} + \frac{\bar{\rho}\epsilon}{\tilde{T}} \geq 0 \quad (28)$$

The modeling assumptions which lead to (28) will be identified below after we consider the turbulent entropy production (in)equality for the unmodeled Reynolds-averaged equations. (28) has the same basic structure associated with the unaveraged Navier-Stokes equations except for the following differences:

1. The entropy \hat{s} is determined from the averaged variables present in our system. This is *not* an average of the instantaneous entropy, rather the entropy associated with the averaging of the instantaneous mass, momentum and energy.
2. The third term on the left-hand side contains not only the divergence of the molecular heat flux but also the divergence of the turbulent heat flux.
3. The first term on the right hand side is the usual viscous dissipation function, $\Upsilon(\tilde{\mathbf{u}}, \tilde{\mathbf{u}})$, which now operates on the averaged velocity field rather than the instantaneous velocity field. The counterpart for the fluctuating velocity field is the last term, i.e.,

$$\bar{\rho}\epsilon = \overline{\Upsilon(\mathbf{u}'', \mathbf{u}'')} \quad (29)$$

where \mathbf{u}'' is the fluctuating velocity relative to the Favre averaged velocity $\tilde{\mathbf{u}}$.

4. The molecular thermal dissipation, $\kappa\tilde{T}_{,i}\tilde{T}_{,i}$, on the right-hand side is augmented with a turbulent thermal dissipation.

A similar (in)equality can be obtained by performing the same operations on the exact unmodeled Reynolds-averaged equations, that is,

$$\begin{aligned} (\bar{\rho}\hat{s})_{,t} + (\bar{\rho}\hat{s}\tilde{u}_i)_{,i} + \left(\frac{-\kappa\tilde{T}_{,i}}{\tilde{T}} \right)_{,i} &= \frac{\Upsilon(\tilde{\mathbf{u}}, \tilde{\mathbf{u}})}{\tilde{T}} + \kappa\frac{\tilde{T}_{,i}\tilde{T}_{,i}}{\tilde{T}^2} + \frac{\bar{\rho}\epsilon}{\tilde{T}} \\ &\quad - \frac{1}{\tilde{T}} \left[\left(\widetilde{\bar{\rho}u_i''e''} \right)_{,i} + \overline{p'u_{i,i}''} \right] \\ &\quad + \frac{1}{\tilde{T}} \left[2\Upsilon(\tilde{\mathbf{u}}, \overline{\mathbf{u}''}) - \overline{pu_{i,i}''} + \left(\kappa\overline{T_{,i}''} \right)_{,i} \right] \end{aligned} \quad (30)$$

where p' is the fluctuating pressure relative to the averaged pressure \bar{p} . Contrasting (28) and (30), the following observations may be made:

1. The averages of the single fluctuations present in the third line of (30) were neglected in the modeling process.
2. The correlation of velocity and internal energy and the correlation of pressure and velocity were modeled by a turbulent conductivity, κ_T , multiplying the mean temperature gradient, i.e.,

$$\left(\widetilde{\bar{\rho}u_i''e''} \right)_{,i} + \overline{p'u_{i,i}''} = \left(\kappa_T\tilde{T}_{,i} \right)_{,i} \quad (31)$$

Any Reynolds-averaged turbulence model of the type considered, satisfying the preceding two conditions, leads to an entropy production (in)equality of the

form (28). As an example of such a model, we may mention the Norris-Reynolds model [25] which we have employed in [24].

Remark

As in the laminar case, the use of turbulent entropy variables (24) results in the satisfaction of a discrete form of the entropy production (in)equality (28) without additional dissipative mechanisms.

6. NUMERICAL EXAMPLES

We present in this section numerical examples that illustrate the behavior of the methods. The finite element spaces were formed by bilinear quadrilaterals and linear triangles and tetrahedra in space and constants in time, where standard quadrature rules were employed for integration in space. Equal-order interpolations were used in all cases.

6.1. One-Dimensional Steady Shock

The methods presented above are conservative for any choice of variables and therefore attain correct shock structure. As an example, a Mach 2 shock is solved on a mesh of 21×1 square elements. The shock is placed at $x = 0$ and the initial conditions are given by

$$x < 0 \quad \begin{cases} M = 2 \\ \rho = 1 \\ u_1 = 1 \\ T = 0.61941 \cdot 10^{-3} \end{cases} \quad x > 0 \quad \begin{cases} M = 0.57735 \\ \rho = 2.66667 \\ u_1 = 0.37500 \\ T = 0.10453 \cdot 10^{-2} \end{cases}$$

The y -velocity component, u_2 , was set to zero in the entire domain. Density, temperature and velocity were specified as boundary conditions at the inflow boundary and temperature at the outflow.

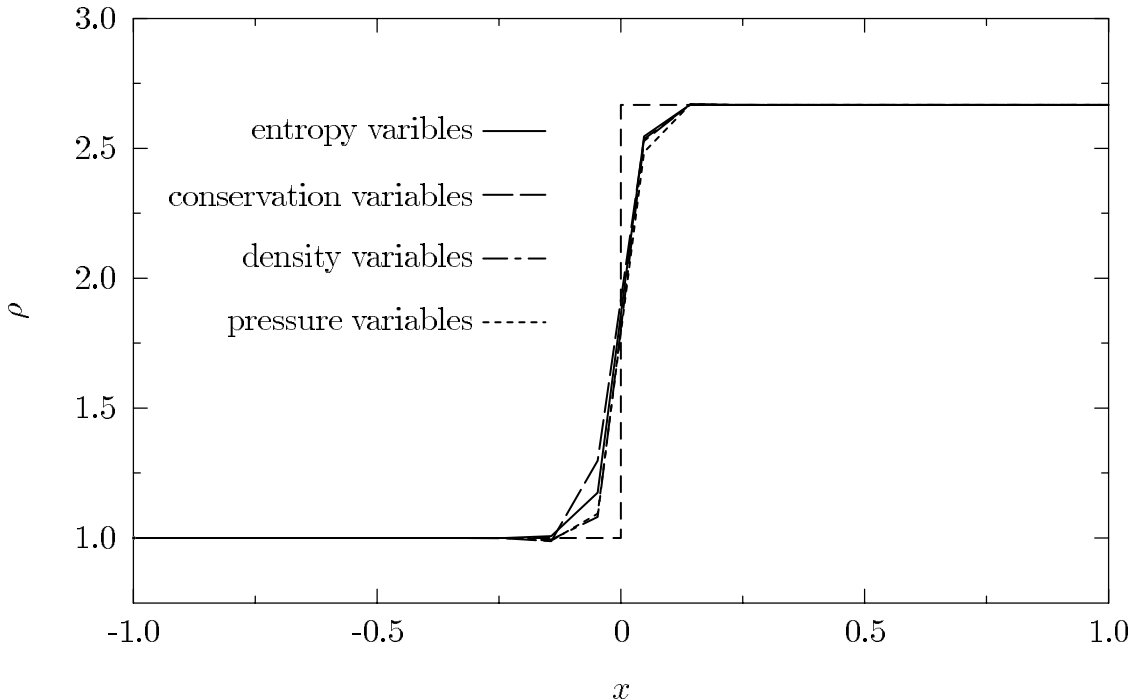


Figure 6. One-dimensional shock.

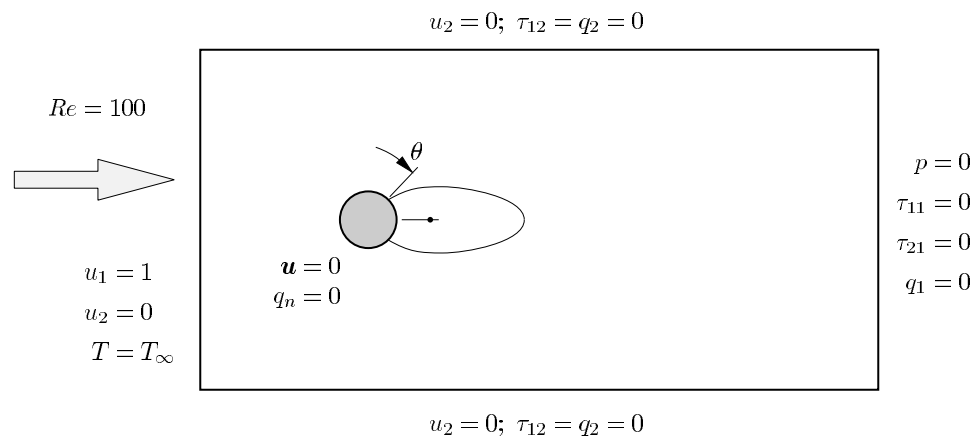


Figure 7. Circular cylinder. Boundary conditions.

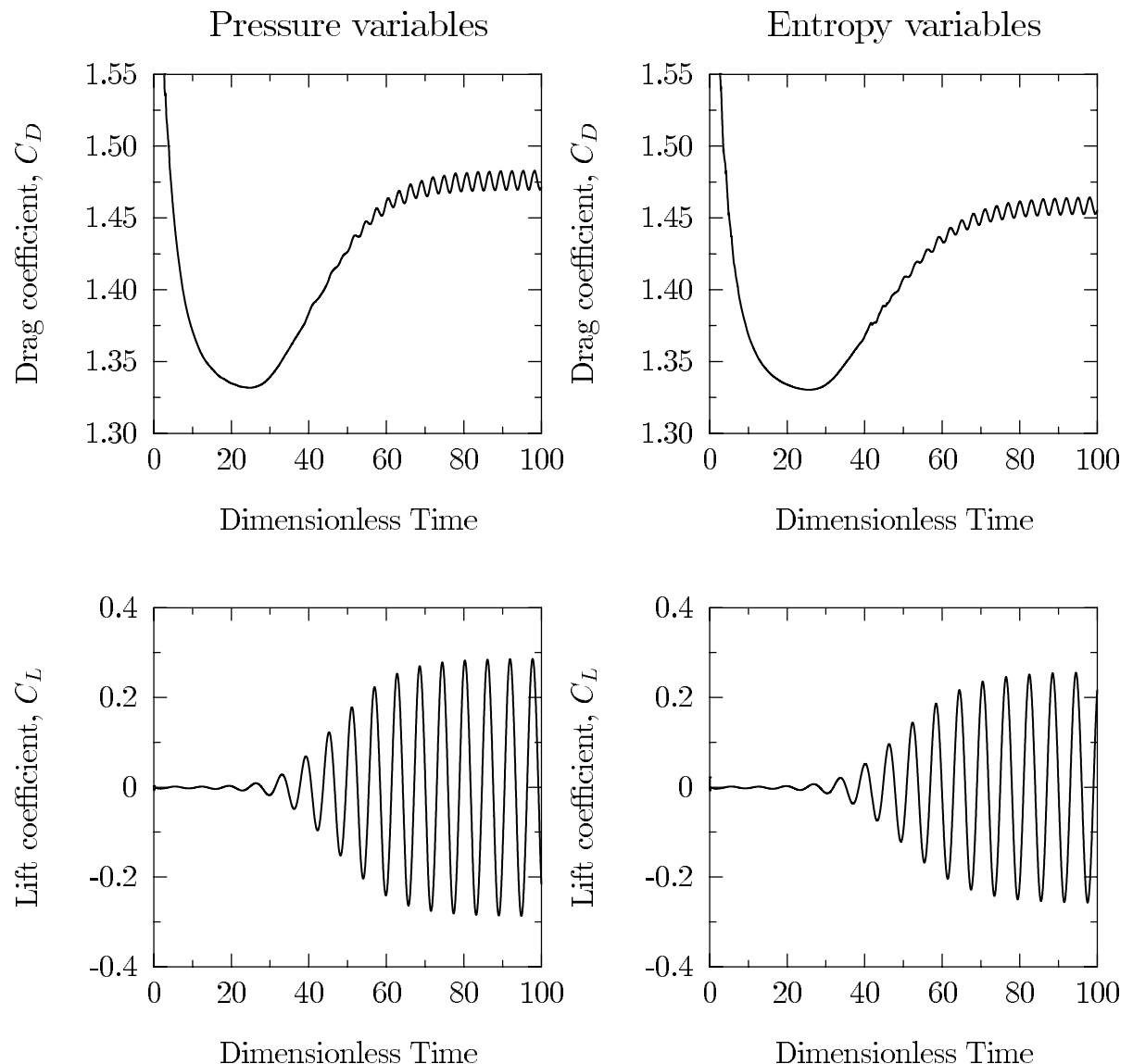


Figure 8. Circular cylinder, $Re = 100$. Evolution of the drag and lift coefficients.

Figure 6 shows the density calculated using several sets of variables, namely, entropy variables, conservations variables, density primitive variables (ρ, \mathbf{u}, T), and pressure primitive variables (p, \mathbf{u}, T). All the methods maintain the correct position and amplitude of the shock. For a nonconservative method the shock will “walk.”

6.2 Circular Cylinder, $Re = 100$

The incompressible flow around a circular cylinder at $Re = 100$ (see Figure 7) leads to a periodic solution, requiring both temporal and spatial accuracy. The time evolution of drag and lift coefficients are compared in Figure 8 for solutions computed with pressure primitive variables and entropy variables. Both sets of variables perform similarly, although there are slight differences in the amplitude of the coefficients and the frequency of the oscillations. Primitive variables yield a Strouhal number of 0.172 for a time step of 0.025, slightly more accurate than 0.166, given by entropy variables.

6.3 Turbulent flow with adverse pressure gradient

The next problem considers turbulent flow in a duct which was studied by Samuel and Joubert [26]; see Figure 9. The changing area of the duct creates an increasingly adverse pressure gradient which in turn dramatically affects the boundary layer and the turbulence within. It should be noted that algebraic models not specifically tuned for this problem are unable to accurately solve it. The coefficient of friction plot shown in Figure 10 compares well with experimental data. For further details, see Jansen *et al.* [24].

6.4 Cylindrical leading edge domain decomposition

Automatic domain decomposition of complex, three-dimensional, adaptively refined meshes is an essential enabling technology for massively parallel computing. As an example of our work in this area, we consider a mesh used by Thareja *et al.* [27] to compute the inviscid shock-shock interaction on a swept cylindrical leading edge (see Figure 11). The mesh is composed of 86,701 tetrahedral elements and 16,707 nodes. Figure 12 illustrates a decomposition of the mesh into 32 subdomains. The quality of the decomposition is excellent even in regions of adaptive refinement. For the Connection Machine CM-5, decompositions require four subdomains for each processing node. Consequently, for large CM-5 systems, decompositions into thousand of subdomains are required. This can represent a significant computational burden if not executed extremely efficiently. In our work, we have developed a parallel implementation of the so-called recursive spectral bisection algorithm developed by Pothen *et al.* [28]. A detailed presentation may be found in Johan *et al.* [20].

6.5 F-18 fighter jet

This last example involves the supersonic inviscid flow at Mach 1.5 around an F-18 fighter jet. The tetrahedral mesh has 182,055 nodes and 1,010,174 elements. The computation ran for 20 time steps at a CFL number of 5 followed by 80 time steps at a CFL number of 10. Entropy variables were employed. The resulting pressure contours on the surface of the airplane are shown in Figure 13. Note that we computed the fluid flow around the complete airplane even though this problem has a plane of symmetry. This problem was solved on a 512-node CM-5 system. Timings are presented in Table 1. Additional speed-ups are to be

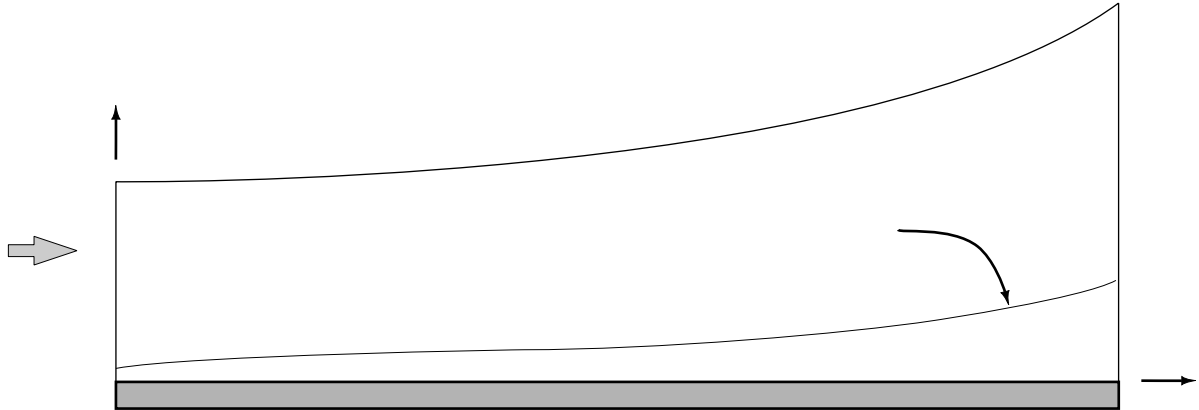


Figure 9. Increasingly adverse pressure gradient flow.

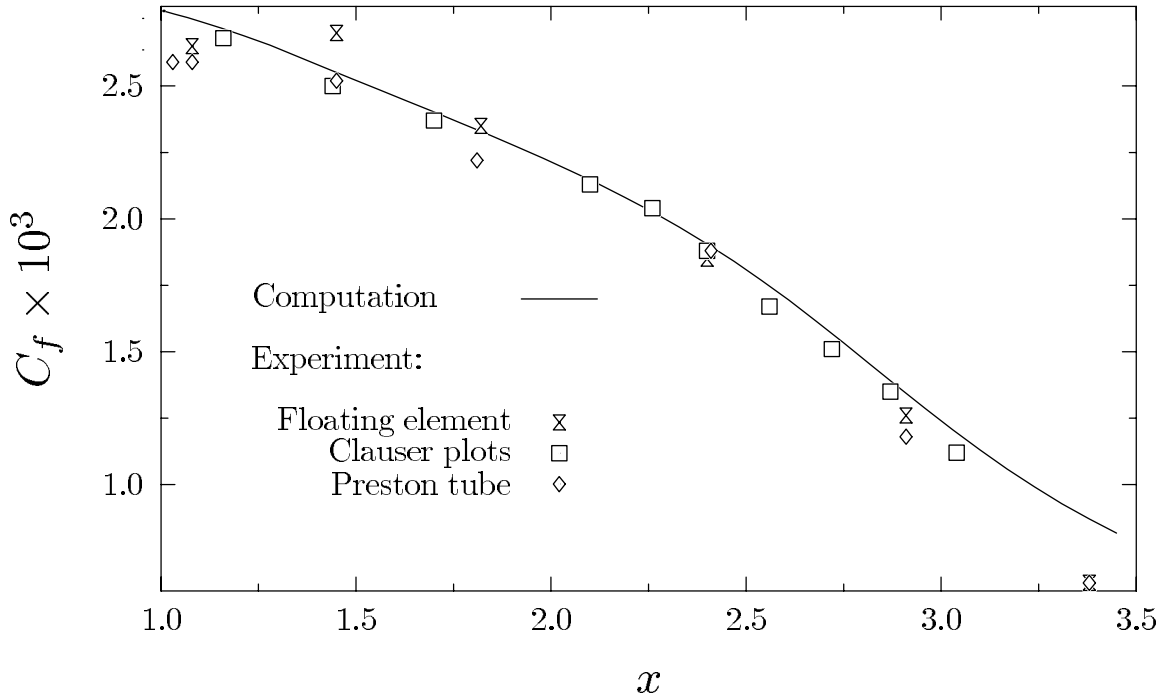


Figure 10. Coefficient of friction for the increasingly adverse pressure gradient flow. The computational results are compared with results for various methods of experimental measurement.

expected before the final release of the CM-5 software. This numerical example also indicates that solving a one million degree of freedom aerodynamic problem in under 10 minutes can be done routinely today on a contemporary parallel computer. The finite element program was clocked at 12.0 Gflops/s on this CM-5 configuration. This rate includes both computation *and* communication, i.e., gather and scatter operations. Communication strategies are described in Johan *et al.* [19, 20].

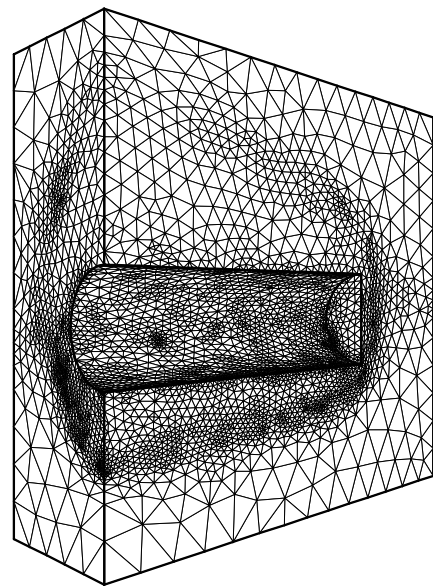


Figure 11. Cylindrical leading edge. View of the surface mesh.

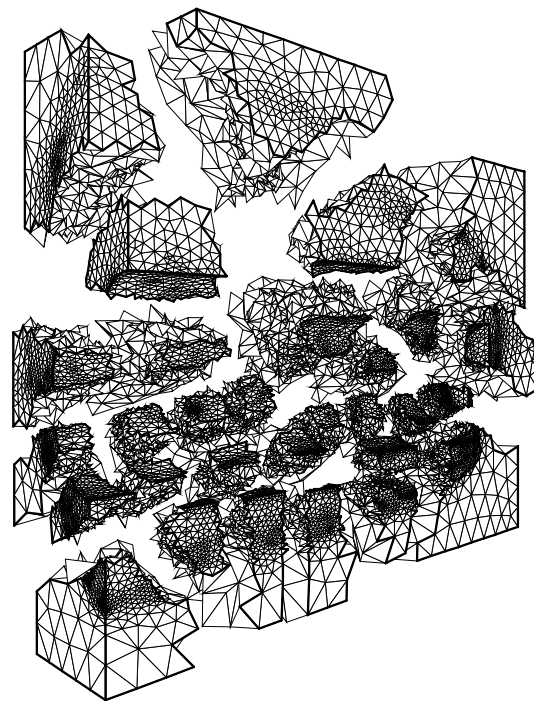


Figure 12. Cylindrical leading edge. Decomposition into 32 partitions.

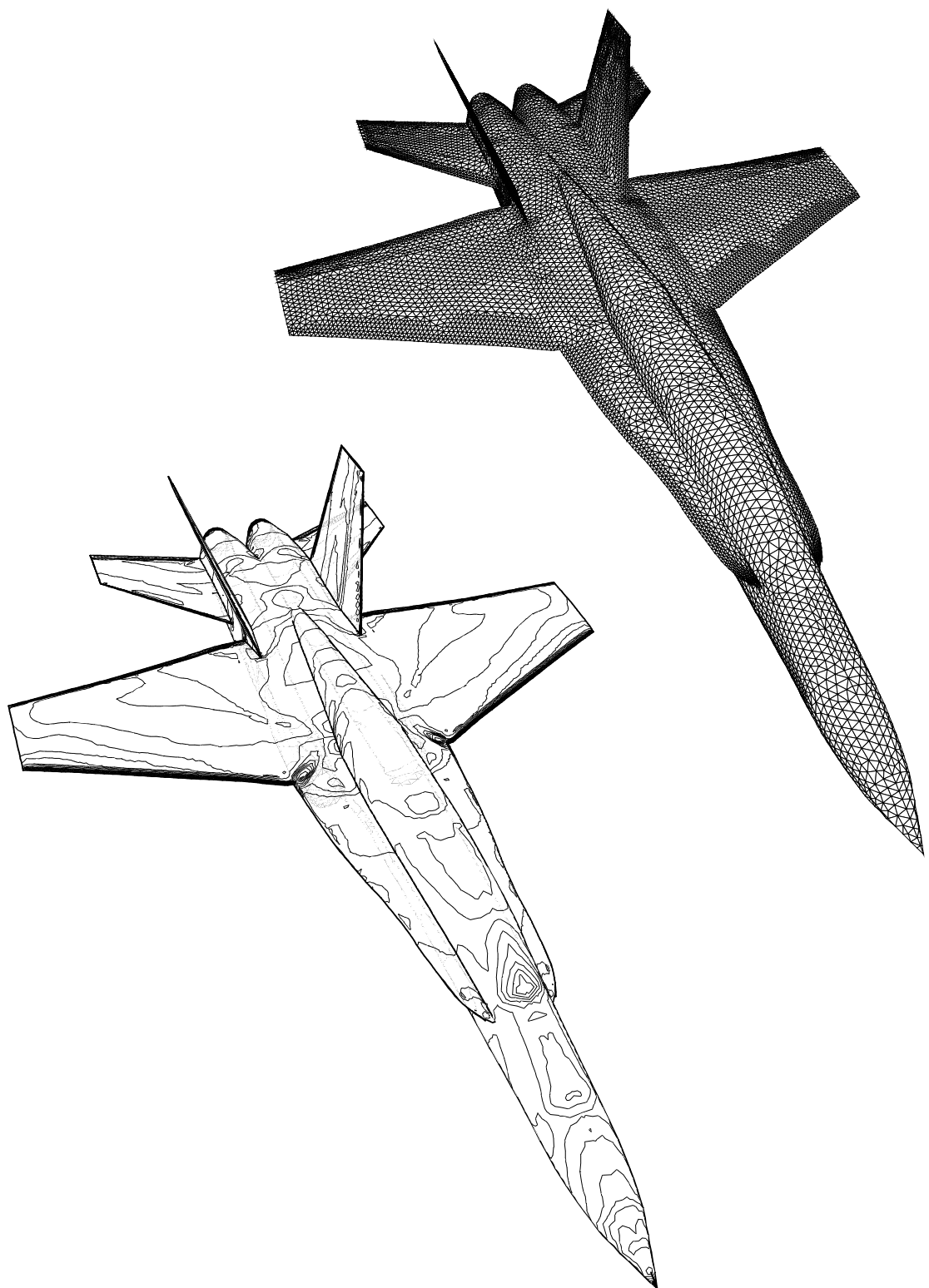


Figure 13. F-18 fighter jet. View of surface mesh and pressure contours.

Table 1. F-18 fighter jet. Times for 100 time steps on a 512-processing node CM-5 system.

Gather operations	43 s
Computation	279 s
Scatter operations	68 s
Total time	6 min 30 s
Solver flop rate	12.0 Gflops/s

7. CONCLUSIONS

We have briefly reviewed the status of stabilized methods in computational fluid dynamics herein. We have also summarized a few current developments. In particular we presented a formulation which accommodates any choice of variables. The basis of the derivation is the entropy variables formulation which has been used with considerable success previously. The change of variables from entropy variables to any other set of variables is performed directly in the variational equation. The discrete Clausius-Duhem (in)equality is satisfied by the choice of entropy variables whether or not additional dissipative mechanisms are present. This is not the case for other choices of variables. However, entropy production is still enforced by the additional dissipative mechanisms present in the formulation, namely, the least-squares term and the discontinuity capturing operator. For any choice of variables, global conservation and correct shock structure are preserved. The approach is stable for any combination of continuous interpolations, in particular, equal-order interpolations. The choices of the primitive variables (p, \mathbf{u}, T) and entropy variables lead to well-posed formulations in the incompressible limit. In this way, one computer program can be written which is applicable to both compressible and incompressible flows.

Extension of our methodology to turbulent flows was also considered. We addressed the Reynolds-averaged Navier-Stokes equations appended with a turbulent kinetic energy transport equation. Turbulent entropy production (in)equalities were derived for the exact Reynolds-averaged equations and ones employing typical modeling assumptions. The entropy production (in)equality represents the fundamental nonlinear stability condition of a turbulence model. It is automatically satisfied in our formulation in direct analogy with the laminar case.

Numerical examples were presented to illustrate the preceding developments. We also presented applications which illustrate current developments on massively parallel computers. Issues such as load balancing and automatic domain decomposition were briefly addressed, and a calculation was presented which illustrates the capabilities of a contemporary machine. We expect significant progress to be made in this area in the immediate future.

ACKNOWLEDGEMENTS

We want to thank Jim Stewart for helpful suggestions. Guillermo Hauke was sponsored by the Ministerio de Educación y Ciencia, Spain. We would like also to express our gratitude to Rajiv Thareja (NASA Langley) for providing us with the cylinder mesh and Jean Cabello and Rainald Löhner (George Washington University) for providing us with the F-18 mesh.

REFERENCES

1. GOUDREAU, G.L. - Evaluation of Discrete Methods for the Linear Dynamic Response of Elastic and Viscoelastic Solids,
UC SESM Report 69-15, University of California, Berkeley, (1970).
2. TAYLOR, R.L. and IDING, R. - Application of Extended Variational Principles to Finite Element Analysis,
Variational methods in Engineering, Vol. I, Southampton University Press, 1973, 2.54-2.67.
3. HILBER, H.M., HUGHES, T.J.R. and TAYLOR, R.L. - Mass Matrices for Improved Finite Element Eigenvalue Approximations,
unpublished report (1975).
4. BROOKS, A.N. and HUGHES, T.J.R. - Streamline Upwind Petrov-Galerkin Formulations for Convection Dominated Flows with Particular Emphasis on the Incompressible Navier-Stokes Equations,
Comput. Methods Appl. Mech. Eng., **32**, 199-259 (1982).
5. HUGHES, T.J.R., FRANCA, L.P. and MALLET, M. - A New Finite Element Formulation for Computational Fluid Dynamics: I. Symmetric Forms of the Compressible Euler and Navier-Stokes Equations and the Second Law of Thermodynamics, *Comp. Methods Appl. Mech. Eng.*, **54**, 223-234 (1986).
6. HUGHES, T.J.R. and MALLET, M. - A New Finite Element Formulation for Computational Fluid Dynamics: III. The Generalized Streamline Operator for Multidimensional Advective-Diffusive Systems,
Comput. Methods Appl. Mech. Eng., **58**, 305-328 (1986).
7. HUGHES, T.J.R. and MALLET, M. - A New Finite Element Formulation for Computational Fluid Dynamics: IV. A Discontinuity-Capturing Operator for Multidimensional Advective-Diffusive Systems,
Comput. Methods Appl. Mech. Eng., **58**, 329-336 (1986).
8. HUGHES, T.J.R., FRANCA, L.P. and HULBERT, G. - A New Finite Element Formulation for Computational Fluid Dynamics: VIII. The Galerkin/least-squares Method for Advective-Diffusive Equations,
Comput. Methods Appl. Mech. Eng., **73**, 173-189 (1989).
9. HUGHES, T.J.R. and TEZDUYAR, T.E. - Finite Element Methods for First-order Hyperbolic Systems with particular Emphasis on the Compressible Euler Equations,
Comput. Methods Appl. Mech. Eng., **45**, 217-284 (1984).

10. HANSBO, P. and JOHNSON, C. - Adaptive Streamline Diffusion Methods for Compressible Flow using Conservation Variables, *Comput. Methods Appl. Mech. Eng.*, **87**, 267-280 (1991).
11. ALIABADI, S.K., RAY, S.E. and TEZDUYAR, T.E. - SUPG Finite Element Computation of Viscous Compressible Flows based on the Conservation and Entropy Variables Formulation, University of Minnesota Supercomputer Institute Research Report UMSI 92/136, 1992.
12. CHALOT, F., HUGHES, T.J.R. and SHAKIB, F. - Symmetrization of Conservation Laws with Entropy for High-temperature Hypersonic Computations, *Comput. Syst. Eng.*, **1**, 495-521 (1990).
- 13 DE GROOT, S.R. and MAZUR, P. - *Non-equilibrium thermodynamics*, Dover Publications, New York (1984).
- 14 JOHNSON, C., NAVERT, U. and PITKÄRANTA, J. - Finite elements methods for linear hyperbolic problems, *Computer Methods in Applied Mechanics and Engineering*, **45** 285–312 (1984).
- 15 LESAINT, P. and RAVIART, P. - On a finite element method for solving the neutron transport equation in: C. de Boor (ed.), *Mathematical Aspects of Finite Elements in Partial Differential Equations*, Academic Press, New York, 89–123, (1974).
- 16 VON NEUMANN J. and RICHTMYER R.D. - A method for the numerical calculation of hydrodynamic shocks, *Journal of Applied Physics*, **21**, 232–237 (1950).
17. SHAKIB, F., HUGHES, T.J.R. and JOHAN, Z. - A New Finite Element Formulation for Computational Fluid Dynamics: X. The Compressible Euler and Navier-Stokes Equations, *Comput. Methods Appl. Mech. Eng.*, **89**, 141-219 (1991).
- 18 SHAKIB, F, HUGHES, T.J.R. and JOHAN, Z. - A multi-element group pre-conditioned GMRES algorithm for nonsymmetric systems arising in finite element analysis, *Computer Methods in Applied Mechanics and Engineering*, **75**, 415–456 (1989).
19. JOHAN, Z., HUGHES, T.J.R., MATHUR, K.K. and JOHNSSON, S.L. - A Data Parallel Finite Element Method for Computational Fluid Dynamics on the Connection Machine System, *Comput. Methods Appl. Mech. Eng.*, **99**, 113-134 (1992).
20. JOHAN, Z., MATHUR, K.K., JOHNSSON, S.L. and HUGHES, T.J.R. - An Efficient Communication Strategy for Finite Element Methods of the Connection Machine CM-5 System, *Comput. Methods Appl. Mech. Eng.*, **113**, 363-387 (1994).

21. HUGHES, T.J.R. - *The Finite Element Method: Linear Static and Dynamic Finite Element Analysis*. Prentice-Hall, Englewood Cliffs, New Jersey, 1987.
22. FAVRE, A. - Equations des Gaz Turbulents Compressibles, *J. de Mécanique*, **4**, 391-421 (1958).
23. VANDROMME, D. - Introduction to Turbulence Modeling, *Von Karman Institute Lecture Series*, 1991-02, Waterloo, Belgium, 1991.
24. JANSEN, K., JOHAN, Z. and HUGHES, T.J.R. - Implementation of a One-equation Turbulence Model Within a Stabilized Finite Element Formulation of a Symmetric Advective-Diffusive System, *Comput. Methods Appl. Mech. Eng.*, **105**, 405-433 (1993).
25. NORRIS, L.H. and REYNOLDS W.C. - Channel Flow with a Moving Wavy Boundary, Report FM-10, Stanford University, Department of Mechanical Engineering, Stanford, 1975.
- 26 SAMUEL, A.E. and JOUBERT, P.N. - A boundary layer developing in an increasingly adverse pressure gradient, *Journal of Fluid Mechanics*, **6**, (1975) 481.
27. THAREJA, R.R., MORGAN, K., PERAIRE, J. and PIERO, J. - A Three-dimensional Upwind Finite Element Point Implicit Unstructured Grid Euler Solver, AIAA 27th Aerospace Sciences Meeting, paper AIAA-89-0658, 1989.
28. POTHEEN, A., SIMON, H.D. and LIOU, K.P. - Partitioning Sparse Matrices With Eigenvectors of Graphs, *SIAM Journal of Matrix Analysis and Applications*, **11**, 430-452 (1990).